

## The Migrastatin Family: Discovery of Potent Cell Migration Inhibitors by Chemical Synthesis

Christoph Gaul, Jn T. Njardarson, Dandan Shan, David C. Dorn, Kai-Da Wu, William P. Tong, Xin-Yun Huang, Malcolm A. S. Moore, and Samuel J. Danishefsky

*J. Am. Chem. Soc.*, **2004**, 126 (36), 11326-11337 • DOI: 10.1021/ja048779q • Publication Date (Web): 30 July 2004

Downloaded from <http://pubs.acs.org> on April 1, 2009

### More About This Article

Additional resources and features associated with this article are available within the HTML version:

- Supporting Information
- Links to the 8 articles that cite this article, as of the time of this article download
- Access to high resolution figures
- Links to articles and content related to this article
- Copyright permission to reproduce figures and/or text from this article

[View the Full Text HTML](#)



## The Migrastatin Family: Discovery of Potent Cell Migration Inhibitors by Chemical Synthesis

Christoph Gaul,<sup>†</sup> Jón T. Njardarson,<sup>†</sup> Dandan Shan,<sup>‡</sup> David C. Dorn,<sup>§</sup> Kai-Da Wu,<sup>§</sup>  
William P. Tong,<sup>||</sup> Xin-Yun Huang,<sup>‡</sup> Malcolm A. S. Moore,<sup>§</sup> and  
Samuel J. Danishefsky<sup>\*,†,⊥</sup>

*Contribution from the Laboratory for Bioorganic Chemistry, Sloan-Kettering Institute for Cancer Research, 1275 York Avenue, New York, New York 10021, Department of Physiology, Weill Medical College of Cornell University, 1300 York Avenue, New York, New York 10021, Laboratory of Developmental Hematopoiesis, Cell Biology Program, Sloan-Kettering Institute for Cancer Research, New York, New York 10021, Analytical Core Facility, Sloan-Kettering Institute for Cancer Research, 1275 York Avenue, New York, New York 10021, and Department of Chemistry, Columbia University, Havemeyer Hall, 3000 Broadway, New York, New York 10027*

Received March 3, 2004; E-mail: s-danishefsky@ski.mskcc.org

**Abstract:** The first asymmetric total synthesis of (+)-migrastatin (**1**), a macrolide natural product with anti-metastatic properties, has been accomplished. Our concise and flexible approach utilized a Lewis acid-catalyzed diene aldehyde condensation (LACDAC) to install the three contiguous stereocenters and the trisubstituted (*Z*)-alkene of migrastatin (**2** + **3** → **21**). Construction of the two remaining stereocenters and incorporation of the glutarimide-containing side chain was achieved by an anti-selective aldol addition of propionyl oxazolidinone **28** to angelic aldehyde **27**, followed by a Horner–Wadsworth–Emmons (HWE) coupling of **32** with glutarimide aldehyde **5**. Finally, the assembly of the macrocycle was realized by a highly (*E*)-selective ring-closing metathesis (**35** → **37**). Utilizing the power of diverted total synthesis (DTS), a series of otherwise inaccessible analogues was prepared and evaluated for their potential as tumor cell migration inhibitors in several in vitro assays. These studies revealed a dramatic increase in activity when the natural motif was considerably simplified, presenting macrolactones **45** and **48**, as well as macrolactam **55**, macroketone **60**, and CF<sub>3</sub>-alcohol **71** as promising anti-metastatic agents.

### Introduction

**Background.** Traditionally, cancer chemotherapy relies on therapeutic agents with cytotoxic properties that inhibit tumor cell proliferation and cause cell death. Recently, the idea of targeting cell migration as an alternative strategy for the development of anti-cancer therapies has generated considerable interest.<sup>1</sup> Intense research efforts are currently directed to the exploration of cell shape change and movement and their underlying mechanisms.<sup>2</sup> Cell migration is involved in a number of physiological processes, including ovulation, embryonic development, tissue regeneration (wound healing), and inflammation. On the other hand, cell migration is also observed in pathological conditions such as tumor angiogenesis, cancer cell invasion, and metastasis.<sup>3</sup> It is believed that primary solid tumors

depend on angiogenesis (formation of new blood vessels) to obtain the necessary oxygen and nutrient supplies for growth beyond a certain size (ca. 1–2 mm). The transition from a pre-angiogenic condition to tumor angiogenesis,<sup>4</sup> often referred to as the angiogenic switch, is followed by tumor growth, cancer cell invasion, and metastasis.<sup>5</sup> In principle, it could be possible to halt (or retard) this procession at different stages with the help of cell migration inhibitors. Because cell migration under ordinary physiological conditions in adults is rather infrequent, its repression might be accompanied by manageable toxicity.

A significant part of our general research program focuses on the development of novel, natural product-inspired anti-cancer agents. These efforts have led to the total chemical synthesis of a number of prominent antitumor natural products,

<sup>†</sup> Laboratory for Bioorganic Chemistry, Sloan-Kettering Institute for Cancer Research.

<sup>‡</sup> Weill Medical College of Cornell University.

<sup>§</sup> Laboratory of Developmental Hematopoiesis, Sloan-Kettering Institute for Cancer Research.

<sup>||</sup> Analytical Core Facility, Sloan-Kettering Institute for Cancer Research.

<sup>⊥</sup> Columbia University.

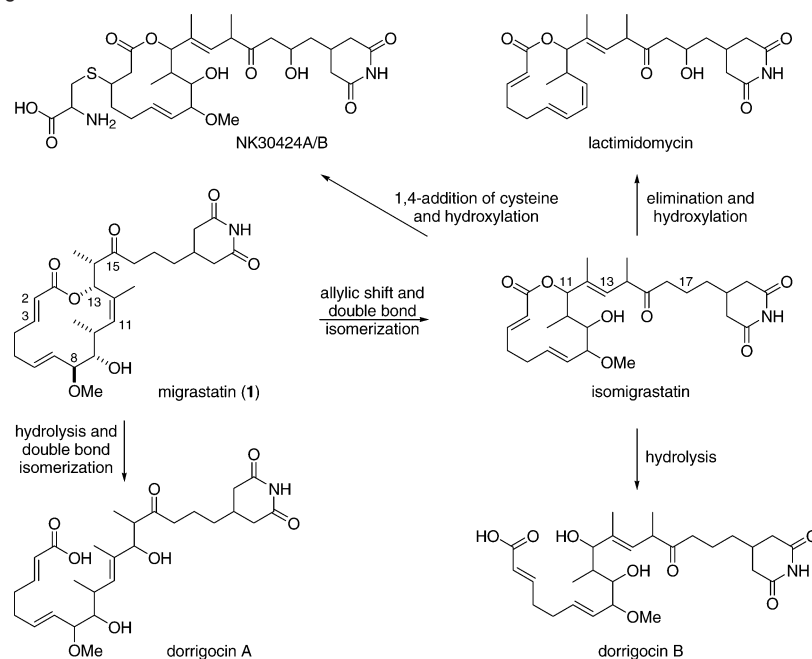
(1) Fenteany, G.; Zhu, S. *Curr. Top. Med. Chem.* **2003**, *3*, 593–616.

(2) Lauffenburger, D. A.; Horwitz, A. F. *Cell* **1996**, *84*, 359–369.

(3) Carmeliet, P. *Nat. Med.* **2003**, *9*, 653–660.

(4) For research efforts toward anti-angiogenic agents, consult: (a) Brower, V. *Nat. Biotechnol.* **1999**, *17*, 963–968. (b) Klohs, W. D.; Hamby, J. M. *Curr. Opin. Biotechnol.* **1999**, *10*, 544–549. (c) Deplanque, G.; Harris, A. L. *Eur. J. Cancer* **2000**, *36*, 1713–1724. (d) Scappaticci, F. A. *J. Clin. Oncol.* **2002**, *20*, 3906–3927. (e) Cristofanilli, M.; Charnsangavej, C.; Hortobagyi, G. N. *Nat. Rev. Drug Discovery* **2002**, *1*, 415–426. (f) Kerbel, R.; Folkman, J. *Nat. Rev. Cancer* **2003**, *2*, 727–739. For early syntheses of natural product angiogenesis inhibitors, see: (g) Corey, E. J.; Snider, B. B. *J. Am. Chem. Soc.* **1972**, *94*, 2549–2550. (h) Corey, E. J.; Dittami, J. P. *J. Am. Chem. Soc.* **1985**, *107*, 256–257. (i) Corey, E. J.; Guzman-Perez, A.; Noe, M. C. *J. Am. Chem. Soc.* **1994**, *116*, 12109–12110.

(5) Woodhouse, E. C.; Chuaqui, R. F.; Liotta, L. A. *Cancer* **1997**, *80* (S8), 1529–1537.

**Scheme 1.** Structure of Migrastatin and Related Natural Products

such as the epothilones,<sup>6</sup> taxol,<sup>7</sup> and, most recently, radicicol<sup>8</sup> and TMC-95A/B.<sup>9</sup> The recent entry of 12,13-desoxyepothilone B (dEpoB), first prepared by total chemical synthesis, into phase II clinical trials,<sup>10</sup> has been followed by the discovery of a new generation of highly potent epothilone analogues.<sup>11</sup> For the most part, our endeavors have converged on cytotoxic agents. The possibility of exploiting natural products as leads for the development of anti-angiogenic and anti-metastatic agents was prompted by the recent isolation and synthesis of compounds such as epoxyquinol A and B,<sup>12</sup> trachyspic acid,<sup>13</sup> azaspirene,<sup>14</sup> evodiamine,<sup>15</sup> motuporamines,<sup>16</sup> borrelidin,<sup>17</sup> and terpestacin.<sup>18</sup>

In particular, a series of independent reports by Imoto<sup>19</sup> and Kosan Bioscience researchers<sup>20</sup> on the discovery of the natural product migrastatin (**1**) enhanced our interest in this area (Scheme 1). It was reported that **1**, isolated from a cultured broth of *Streptomyces*, has the potential of metastasis suppression through its ability to inhibit tumor cell migration. Although the reported activity of migrastatin in a wound-healing assay was rather modest (IC<sub>50</sub> value of 29 μM), we considered it as an attractive lead compound in the search for other, more potent agents. The structure of migrastatin (**1**), determined by X-ray crystal structure analysis, features a 14-membered macrolactone

- (6) For comprehensive reviews, see: (a) Harris, C. R.; Danishefsky, S. J. *J. Org. Chem.* **1999**, *64*, 8434–8456. (b) Stachel, S. J.; Biswas, K.; Danishefsky, S. J. *Curr. Pharm. Des.* **2001**, *7*, 1277–1290.
- (7) Danishefsky, S. J.; Masters, J. J.; Young, W. B.; Link, J. T.; Snyder, L. B.; Magee, T. V.; Jung, D. K.; Isaacs, R. C. A.; Bornmann, W. G.; Alaimo, C. A.; Coburn, C. A.; DiGrandi, M. J. *J. Am. Chem. Soc.* **1996**, *118*, 2843–2859.
- (8) For the synthesis and biological evaluation of radicicol and cyclopropyl-radicicol, see: (a) Garbaccio, R. M.; Stachel, S. J.; Baeschlin, D. K.; Danishefsky, S. J. *J. Am. Chem. Soc.* **2001**, *123*, 10903–10908. (b) Yamamoto, K.; Garbaccio, R. M.; Stachel, S. J.; Solit, D. B.; Chiosis, G.; Rosen, N.; Danishefsky, S. J. *Angew. Chem., Int. Ed.* **2003**, *42*, 1280–1284. (c) Yang, Z. Q.; Danishefsky, S. J. *J. Am. Chem. Soc.* **2003**, *125*, 9602–9603.
- (9) For the synthesis and evaluation of TMC-95A/B, see: (a) Lin, S.; Danishefsky, S. J. *Angew. Chem., Int. Ed.* **2001**, *40*, 512–515. (b) Yang, Z. Q.; Kwok, B. H.; Lin, S.; Koldobskiy, M. A.; Crews, C. M.; Danishefsky, S. J. *ChemBiochem* **2003**, *6*, 508–513.
- (10) For more information about clinical trials of dEpoB, visit: [www.kosan.com](http://www.kosan.com).
- (11) For the synthesis and biological evaluation of recent epothilone analogues, see: (a) Rivkin, A.; Yoshimura, F.; Gabarda, A. E.; Chou, T. C.; Dong, H.; Tong, W. P.; Danishefsky, S. J. *J. Am. Chem. Soc.* **2003**, *125*, 2899–2901. (b) Yoshimura, F.; Rivkin, A.; Gabarda, A. E.; Chou, T. C.; Dong, H.; Sukenick, G.; Morel, F. F.; Taylor, R. E.; Danishefsky, S. J. *Angew. Chem., Int. Ed.* **2003**, *42*, 2518–2521.
- (12) For the isolation of epoxyquinol A and B, see: (a) Kakeya, H.; Onose, R.; Koshino, H.; Yoshida, A.; Kobayashi, K.; Kageyama, S. I.; Osada, H. *J. Am. Chem. Soc.* **2002**, *124*, 3496–3497. (b) Kakeya, H.; Onose, R.; Yoshida, A.; Koshino, H.; Osada, H. *J. Antibiot.* **2002**, *55*, 829–831. For the synthesis of epoxyquinol A and B, see: (c) Shoji, M.; Yamaguchi, J.; Kakeya, H.; Osada, H.; Hayashi, Y. *Angew. Chem., Int. Ed.* **2002**, *41*, 3192–3194. (d) Chaomin, L.; Bardhan, S.; Pace, E. A.; Liang, M. C.; Gilmore, T. D.; Porco, J. A., Jr. *Org. Lett.* **2002**, *4*, 3267–3270. (e) Mehta, G.; Islam, K. *Tetrahedron Lett.* **2003**, *44*, 3569–3572.
- (13) For the isolation of trachyspic acid, see: (a) Shiozawa, H.; Takahashi, M.; Takatsu, T.; Kinoshita, T.; Tanzawa, K.; Hosoya, T.; Furuya, K.; Furihata, K.; Seto, H. *J. Antibiot.* **1995**, *48*, 357–362. For the synthesis of trachyspic acid, see: (b) Hirai, K.; Ooi, H.; Esumi, T.; Iwabuchi, Y.; Hatakeyama, S. *Org. Lett.* **2003**, *5*, 857–859.
- (14) For the isolation of azaspirene, see: (a) Asami, Y.; Kakeya, H.; Onose, R.; Yoshida, A.; Matsuzaki, H.; Osada, H. *Org. Lett.* **2002**, *4*, 2845–2848. For the synthesis of azaspirene, see: (b) Hayashi, Y.; Shoji, M.; Yamaguchi, J.; Sato, K.; Yamaguchi, S.; Mukaiyama, T.; Sakai, K.; Asami, Y.; Kakeya, H.; Osada, H. *J. Am. Chem. Soc.* **2002**, *124*, 12078–12079.
- (15) A screening approach revealed evodiamine as a potent anti-invasive and anti-metastatic agent: (a) Ogasawara, M.; Matsubara, T.; Suzuki, H. *Biol. Pharm. Bull.* **2001**, *24*, 720–723. (b) Ogasawara, M.; Matsubara, T.; Suzuki, H. *Biol. Pharm. Bull.* **2001**, *24*, 917–920. (c) Ogasawara, M.; Matsunaga, T.; Takahashi, S.; Saiki, I.; Suzuki, H. *Biol. Pharm. Bull.* **2002**, *25*, 1491–1493.
- (16) For the isolation, synthesis, and discussion of the anti-angiogenic properties of the motuporamines, see: (a) Williams, D. E.; Lassota, P.; Andersen, R. J. *J. Org. Chem.* **1998**, *63*, 4838–4841. (b) Roskelley, C. D.; Williams, D. E.; McHardy, L. M.; Leong, K. G.; Troussard, A.; Karsan, A.; Andersen, R. J.; Dedhar, S.; Roberge, M. *Cancer Res.* **2001**, *61*, 6788–6794. (c) Williams, D. E.; Craig, K. S.; Patrick, B.; McHardy, L. M.; van Soest, R.; Roberge, M.; Andersen, R. J. *J. Org. Chem.* **2002**, *67*, 245–258.
- (17) For the discovery of the anti-angiogenic properties of borrelidin, see: (a) Wakabayashi, T.; Kageyama, R.; Naruse, N.; Tsukahara, N.; Funahashi, Y.; Kitoh, K.; Watanabe, Y. *J. Antibiot.* **1997**, *50*, 671–676. For the synthesis of borrelidin, see: (b) Duffey, M. O.; LeTiran, A.; Morken, J. P. *J. Am. Chem. Soc.* **2003**, *125*, 1458–1459.
- (18) For the discovery of the anti-angiogenic properties of terpestacin, see: (a) Jung, H. J.; Lee, H. B.; Kim, C. J.; Rho, J. R.; Shin, J.; Kwon, H. J. *J. Antibiot.* **2003**, *56*, 492–496. For the synthesis of terpestacin, see: (b) Tatsuta, K.; Masuda, N. *J. Antibiot.* **1998**, *51*, 602–606. (c) Myers, A. G.; Siu, M.; Ren, F. J. *J. Am. Chem. Soc.* **2002**, *124*, 4230–4232. (d) Chan, J.; Jamison, T. F. *J. Am. Chem. Soc.* **2003**, *125*, 11514–11515.
- (19) (a) Nakae, K.; Yoshimoto, Y.; Sawa, T.; Homma, Y.; Hamada, M.; Takeuchi, T.; Imoto, M. *J. Antibiot.* **2000**, *53*, 1130–1136. (b) Nakae, K.; Yoshimoto, Y.; Ueda, M.; Sawa, T.; Takahashi, Y.; Naganawa, H.; Takeuchi, T.; Imoto, M. *J. Antibiot.* **2000**, *53*, 1228–1230. (c) Takemoto, Y.; Nakae, K.; Kawatani, M.; Takahashi, Y.; Naganawa, H.; Imoto, M. *J. Antibiot.* **2001**, *54*, 1104–1107. (d) Nakamura, H.; Takahashi, Y.; Naganawa, H.; Nakae, K.; Imoto, M.; Shiro, M.; Matsumura, K.; Watanabe, H.; Kitahara, T. *J. Antibiot.* **2002**, *55*, 442–444.
- (20) Woo, E. J.; Starks, C. M.; Carney, J. R.; Arslanian, R.; Cadapan, L.; Zavala, S.; Licari, P. *J. Antibiot.* **2002**, *55*, 141–146.

with a characteristic glutarimide-containing side chain. Embedded in the macrocycle are a trisubstituted (*Z*)-alkene and two disubstituted (*E*)-alkenes, as well as three contiguous stereocenters. The side chain projecting from the cyclic core is associated with stereogenic centers at C13 and C14.

Upon reviewing the literature in search of glutarimide-containing natural products, one encounters prominent examples such as cycloheximide (CHX),<sup>21</sup> streptimidone,<sup>22</sup> and thalidomide, which has resurfaced recently as an anti-angiogenic agent despite its controversial history!<sup>23</sup> Moreover, a number of structural homologues of migrastatin, lactimidomycin,<sup>24</sup> dorrigocin A and B,<sup>20,25</sup> isomigrastatin,<sup>20</sup> and NK30424A/B,<sup>26</sup> have been discovered (Scheme 1). In 1992, lactimidomycin was isolated from *Streptomyces amphibiosporus* and characterized by researchers at Bristol-Myers Squibb. This unique triene-containing 12-membered macrolactone antibiotic is highly cytotoxic in vitro against a number of tumor cell lines and displays in vivo antitumor activity in mice. In addition, lactimidomycin exhibits potent anti-fungal properties and acts as an inhibitor of DNA and protein synthesis. Two years later, the isolation of dorrigocin A and its allylic isomer dorrigocin B from *Streptomyces platensis* was described by researchers at Abbott Laboratories. The dorrigocins are linear polyketide carboxylic acids with a functional group arrangement closely related to migrastatin and isomigrastatin, respectively. They were found to reverse the morphology of *ras*-transformed NIH/3T3 cells from a transformed phenotype to a normal one. Dorrigocin A was also reported to be the first natural product inhibitor of the carboxyl methyltransferase involved in Ras processing. In 2002, the dorrigocins were again isolated from *Streptomyces platensis* by researchers at Kosan Biosciences along with migrastatin and a new member of the family, isomigrastatin. Structurally, isomigrastatin can be described as being derived from migrastatin by an allylic transposition (C13 → C11) and a concomitant double bond isomerization. Thus, isomigrastatin is a 12-membered macrolactone with an exocyclic trisubstituted (*E*)-alkene. The Kosan researchers have shown that the hydrolysis of isomigrastatin leads to dorrigocin B, whereas the hydrolysis of migrastatin produces a geometric isomer of dorrigocin A. The biological profile of isomigrastatin has not been reported to date. The latest members of the glutarimide-containing macrolide family are the natural products NK30424A and its stereoisomer NK30424B, isolated from *Streptomyces* sp.

NA30424 by researchers at Nippon Kayaku. Furthermore, four related compounds, derived from oxidation of the thioether to the sulfoxide, were detected as minor constituents in the cultured broth and were titled as NK30424AS1-2 and NK30424BS1-2. The NK compounds are formally derived from isomigrastatin by conjugate addition of cysteine to the C2–C3 double bond and hydroxylation at C17. Interestingly, these NK congeners are reported to be very potent inhibitors of lipopolysaccharide-induced tumor necrosis factor- $\alpha$  (TNF- $\alpha$ ) promoter activity. To date, migrastatin is the only member of the natural product family described above in which the relative and absolute configurations have been determined. Possibly, total chemical synthesis might aid in deciphering the stereochemistry of other members of this series.

Our research plan for evaluating the migrastatins as anti-metastatic agents comprises the following key stages: A total synthesis of **1** would afford our laboratory with material for an independent evaluation of the biology of the natural product and with opportunities through standard medicinal chemistry for gaining access to a broad range of structural analogues. Moreover, by diversion of the route of total synthesis, we could be in a position to explore structural types that could not, plausibly, be accessible by chemical modification of migrastatin itself. In vitro screening of migrastatin derivatives in cell migration assays could lead to an informative structure–activity relationship (SAR) profile, conceivably assisting in the emergence of compounds with improved biological profiles for progression to in vivo models. Furthermore, efforts directed at target identification are expected to yield some insight into the biological mode of action of migrastatin and its congenitors.

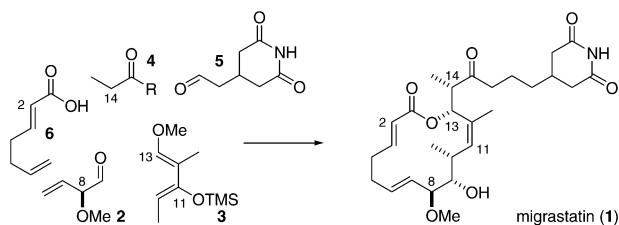
Previously, we have communicated a total synthesis of migrastatin<sup>27</sup> and preliminary SAR studies.<sup>28</sup> In this paper, we provide a full account of the synthetic endeavor, which resulted in an efficient and flexible total synthesis of **1**. In addition, we detail the preparation and biological evaluation of an extended, diverse set of migrastatin analogues which led to the discovery of highly potent cell migration inhibitors. We also describe our undertakings to address issues of in vivo evaluation (large-scale preparation of analogues), metabolic stability studies, and target identification (labeling). In short, we show how the science of total synthesis can be integrated into the progression of drug discovery.

**Synthetic Plan.** It was particularly important to devise a concise, flexible, and readily scaleable synthesis, since it would remain for synthesis to fuel an aggressive SAR elucidation program and to provide significant quantities of materials for in vivo studies. This is in keeping with the notion that total synthesis was viewed as a first milestone of the project, rather than as an end-point.

Any synthetic plan directed at migrastatin, and seeking to meet the standards discussed above, must address several obvious structural issues. Clearly, accommodation must be provided for the (*E*)-configuration of the C2–C3 and C6–C7 double bonds, as well as for the (*Z*)-configuration of the C11–C12 double bond of the trienic lactone. Moreover, protocols are required for maintaining stereocontrol over the dispositions of the stereogenic centers at C8, C9, C10, and C13. In addition,

- (21) Cycloheximide (CHX) is a glutarimide antibiotic that inhibits protein synthesis. CHX is widely used for studies of cell death and is commercially available as Ready Made solution by Sigma. For a more recent leading article, see: Mattson, M. P.; Furukawa, K. *Apoptosis* **1997**, *2*, 257–264.
- (22) For a recent synthesis of streptimidone, a glutarimide antibiotic, see: Kondo, H.; Oritani, T.; Kiyota, H. *Eur. J. Org. Chem.* **2000**, 3459–3462.
- (23) For the original discovery of the anti-angiogenic properties of thalidomide, see: (a) D'Amato, R. J.; Loughnan, M. S.; Flynn, E.; Folkman, J. *Proc. Natl. Acad. Sci. U.S.A.* **1994**, *91*, 4082–4085. For recent discussions of the use of thalidomide in anti-cancer therapy, see: (b) Thomas, D. A.; Kantarjian, H. M. *Curr. Opin. Oncol.* **2000**, *12*, 564–573. (c) Raje, N.; Anderson, K. C. *Curr. Opin. Oncol.* **2002**, *14*, 635–646. (d) Dredge, K.; Dalgleish, A. G.; Marriott, J. B. *Anti-Cancer Drugs* **2003**, *14*, 331–335. (e) Capitosti, S. M.; Hansen, T. P.; Brown, M. L. *Bioorg. Med. Chem.* **2004**, *12*, 327–336.
- (24) Sugawara, K.; Nishiyama, Y.; Toda, S.; Komiyama, N.; Hatori, M.; Moriyama, T.; Sawada, Y.; Kamei, H.; Konishi, M.; Oki, T. *J. Antibiot.* **1992**, *45*, 1433–1441.
- (25) (a) Karwowski, J. P.; Jackson, M.; Sunga, G.; Sheldon, P.; Poddig, J. B.; Kohl, W. L.; Adam, S. *J. Antibiot.* **1994**, *47*, 862–869. (b) Hochlowski, J. E.; Whitern, D. N.; Hill, P.; McAlpine, J. B. *J. Antibiot.* **1994**, *47*, 870–874. (c) Kadam, S.; McAlpine, J. B. *J. Antibiot.* **1994**, *47*, 875–880.
- (26) (a) Takayasu, Y.; Tsuchiya, K.; Aoyama, T.; Sukenaga, Y. *J. Antibiot.* **2001**, *54*, 1111–1115. (b) Takayasu, Y.; Tsuchiya, K.; Sukenaga, Y. *J. Antibiot.* **2002**, *55*, 337–340.

- (27) Gaul, C.; Njardarson, J. T.; Danishefsky, S. J. *J. Am. Chem. Soc.* **2003**, *125*, 6042–6043.
- (28) Njardarson, J. T.; Gaul, C.; Shan, D.; Huang, X. Y.; Danishefsky, S. J. *J. Am. Chem. Soc.* **2004**, *126*, 1038–1040.

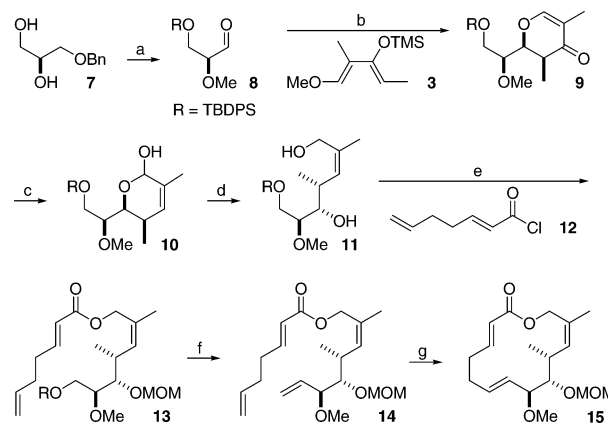
**Scheme 2.** Strategy for the Assembly of Migrastatin

it is necessary to accomplish an installation of the required side chain projecting from C13 and the inclusion of the stereocenter at C14, which is not part of the ring structure. Needless to say, suitable provision is needed for the incorporation of the C15 keto group as well as the  $\delta$ -substituted glutarimide at C18.

A comprehensive plan that embraces these structural issues is suggested in Scheme 2. Our retrosynthetic analysis led us back to the five components **2**, **3**, **4**, **5**, and **6** shown therein. The (*E*)-geometric character of the C2–C3 double bond could be secured via recourse to the known compound **6**. A key feature of this synthesis would be the use of aldehyde **2**, bearing the methoxy-substituted stereogenic center, ultimately to be emplaced at C8. Another important building block would be diene **3**. This type of synergistically activated, dibranched, bisoxygenated butadiene was part of our all-carbon Diels–Alder research in the mid 1970s.<sup>29</sup> Indeed, in the 1980s, this type of diene was used in the context of our LACDAC chemistry to create dihydropyrans.<sup>30</sup> The aldehyde in this case would be the previously discussed **2**. Appropriate disconnection of the pyran would expose the four-carbon segment comprising C10–C13. The two methyl-branching elements of **3** would appear at C10 and C12 in migrastatin following appropriate manipulations. At the outset, the precise nature of the R function in keto building block **4** awaited specification. The decisive criterion for various candidate structures that might be interrogated would be their amenability to linkage to the emerging C13 in the context of macrolactone formation, while enabling smooth incorporation of the  $\delta$ -branched glutarimide. We note that the sum of fragments **2** and **6** contains two carbons in excess of those required for formation of the 14-membered macrolactone. Such a disconnection invited the prospect of establishing this lactone through a ring-closing metathesis (RCM) reaction with extrusion of the two seemingly extraneous carbon centers. A more detailed analysis of the synthetic issues appears in the context of the next section, in which we describe the implementation of the broad plan.

## Results and Discussion

**Model Study.** It seemed prudent to assess, in the context of a model study, the feasibility of RCM to construct the 14-membered ring of migrastatin (Scheme 3).<sup>31</sup> In this connection, we would also address the stereoselectivity (geometry of the C6–C7 double bond) and chemoselectivity (undesired RCM-participation of the C2–C3 and C11–C12 double bonds) of the ring-closing reaction. Such questions were to be first posed in a study directed to the synthesis of the migrastatin core structure lacking the glutarimide-containing side chain.

**Scheme 3.** A Model Study: Synthesis of the Migrastatin Core **15**<sup>a</sup>

<sup>a</sup> Reagents and conditions: (a) (i) TBDPSCl, imidazole, DMF, room temperature, (ii) MeI, NaH, THF, room temperature, (iii) H<sub>2</sub>, Pd(OH)<sub>2</sub>, EtOAc, room temperature, (iv) (COCl)<sub>2</sub>, Et<sub>3</sub>N, DMSO, CH<sub>2</sub>Cl<sub>2</sub>, –78 °C to room temperature, 66%; (b) (i) TiCl<sub>4</sub>, CH<sub>2</sub>Cl<sub>2</sub>, –78 °C, (ii) TFA, CH<sub>2</sub>Cl<sub>2</sub>, room temperature, 79%; (c) (i) NaBH<sub>4</sub>, CeCl<sub>3</sub>·7H<sub>2</sub>O, EtOH, 0 °C, (ii) CSA, H<sub>2</sub>O, THF, reflux; (d) LiBH<sub>4</sub>, H<sub>2</sub>O, THF, room temperature, 55% from **9**; (e) (i) DMAP, CH<sub>2</sub>Cl<sub>2</sub>, room temperature, (ii) MOMCl, Bu<sub>4</sub>NI, *i*-Pr<sub>3</sub>NEt, CH<sub>2</sub>Cl<sub>2</sub>, room temperature, 57%; (f) (i) HF-pyridine, THF, room temperature, (ii) Dess–Martin periodinane, CH<sub>2</sub>Cl<sub>2</sub>, room temperature, (iii) Tebbe reagent, pyridine, THF, –78 to –10 °C, 54%; (g) Grubbs-II catalyst **16** (20 mol %), toluene (0.5 mM), reflux, 50%.

Because we were concerned about the stability, stereochemical integrity, and potential volatility of the previously unknown  $\alpha$ -methoxy- $\alpha$ -vinyl aldehyde **2** (Scheme 2) contemplated for the LACDAC reaction, we began, in this testing phase, with the structurally less challenging heterodienophilic siloxy-aldehyde **8** (Scheme 3). This compound was prepared from commercially available (*S*)-3-benzyloxy-1,2-propanediol **7**<sup>32</sup> in four steps. The sterically demanding TBDPS protecting group was chosen with a view toward suppressing a possible  $\beta$ -chelation pathway relative to the desired  $\alpha$ -chelation mode in the LACDAC sequence. Earlier research of Reetz<sup>33</sup> provided a suggestion that oxygen chelation effects in the control of diastereofacial reactions are suppressed in bulky silyl ether settings.

Indeed, as intended, reaction of aldehyde **8** and diene **3**<sup>34</sup> under the influence of TiCl<sub>4</sub> yielded the  $\alpha$ -chelation controlled product **9** (Scheme 3).<sup>35</sup> Treatment of dihydropyrone **9** with NaBH<sub>4</sub> and CeCl<sub>3</sub>·7H<sub>2</sub>O (Luche reduction)<sup>36</sup> led to the corresponding 1,2-reduced compound, which underwent a Ferrier rearrangement<sup>37</sup> in aqueous acidic THF to produce lactol **10**, with the desired (*Z*)-olefin now in place. Reductive opening of lactol **10** with LiBH<sub>4</sub> afforded diol **11** in 55% overall yield from dihydropyrone **9**. The primary hydroxyl group of **11** was selectively acylated with 2,6-heptadienoyl chloride **12**,<sup>38</sup> and,

(29) Danishefsky, S. J.; Kitahara, T. *J. Am. Chem. Soc.* **1974**, *96*, 7807–7808.

(30) (a) Danishefsky, S. J. *Aldrichimica Acta* **1986**, *19*, 59–69. (b) Danishefsky, S. J. *Chemtracts* **1989**, *2*, 273–297.

(31) Gaul, C.; Danishefsky, S. J. *Tetrahedron Lett.* **2002**, *43*, 9039–9042.

(32) (*S*)-3-benzyloxy-1,2-propanediol **7** is commercially available (Fluka, Aldrich), but only at a high cost. Compound **7** can be easily prepared from inexpensive starting materials: (a) Xiang, G.; McLaughlin, L. W. *Tetrahedron* **1998**, *54*, 375–392. (b) Kitaori, K.; Furukawa, Y.; Yoshimoto, H.; Otera, J. *Tetrahedron* **1999**, *55*, 14381–14390.

(33) Reetz, M. T.; Kessler, K. *J. Org. Chem.* **1985**, *50*, 5434–5436.

(34) Danishefsky, S. J.; Yan, C. F.; Singh, R. K.; Gammill, R. B.; McCurry, P. M., Jr.; Fritsch, N.; Clardy, J. *J. Am. Chem. Soc.* **1979**, *101*, 7001–7008.

(35) For chelation-controlled cyclocondensations of  $\alpha$ -alkoxy aldehydes with synergistically activated dienes, see: Danishefsky, S. J.; Pearson, W. H.; Harvey, D. F.; Maring, C. J.; Springer, J. P. *J. Am. Chem. Soc.* **1985**, *107*, 1256–1268.

(36) Luche, J. L.; Gemal, A. L. *J. Am. Chem. Soc.* **1979**, *101*, 5848–5849.

(37) Ferrier, R. J. *J. Chem. Soc.* **1964**, 5443–5450.

(38) (a) Katzenellenbogen, J. A.; Crumrine, A. L. *J. Am. Chem. Soc.* **1976**, *98*, 4925–4935. (b) Ahmar, M.; Duyck, C.; Fleming, I. *J. Chem. Soc., Perkin Trans. 1* **1998**, 2721–2732.

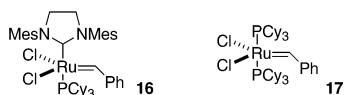


**Figure 1.** Structures of the Grubbs-II (**16**) and Grubbs-I (**17**) catalysts.

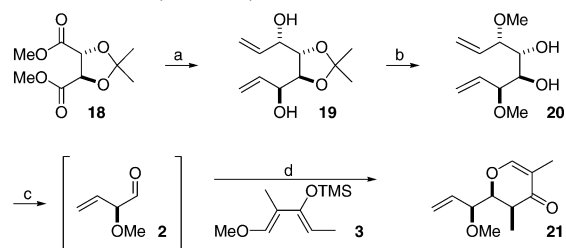
thereafter, the secondary hydroxyl group in the acylation product was protected as its MOM ether.

The RCM precursor **14** was reached from **13** through a three-step sequence, consisting of deprotection, oxidation, and Tebbe olefination.<sup>39</sup> When tetraene **14** was subjected to the action of Grubbs catalyst **16**<sup>40</sup> (Figure 1) in refluxing toluene,<sup>41</sup> the 14-membered macrolactone **15** was generated as the desired (*E*)-congener in 50% yield. Competitive participation of the electron-poor C2–C3 double bond and the sterically hindered C11–C12 double bond in the metathesis step could not be detected. Interestingly, treatment of **14** with Grubbs-I catalyst **17** (Figure 1) in refluxing CH<sub>2</sub>Cl<sub>2</sub> led exclusively to the dimeric product derived from cross metathesis of the terminal double bond of the acyl moiety.

**Synthesis of Key Intermediate 26.** The model study demonstrated the efficacy of the LACDAC sequence to construct the three stereocenters C8–C10 and the power of RCM to establish the macrocyclic system. Encouraged by these early results, we embarked on the total synthesis of migrastatin. Prior to facing the unresolved issues of building up the remaining stereocenters at C13 and C14 in the context of emplacement of the glutarimide moiety, we addressed an issue of process, asking the question whether  $\alpha$ -methoxy- $\alpha$ -vinyl aldehyde **2** might indeed serve as a suitable heterodienophile in the reaction with diene **3** after all. Utilization of aldehyde **2** in the LACDAC reaction would allow us to streamline the synthesis in a most useful way by avoiding the chemistry needed to incorporate the C6–C7 double bond required for RCM.

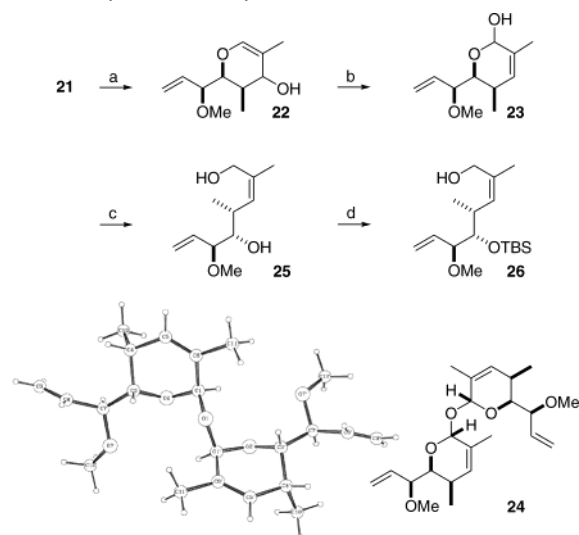
Happily, we could gain an excellent entry into this type of aldehyde, starting from commercially available dimethyl 2,3-*O*-isopropylidene-*L*-tartrate **18** (Scheme 4). Toward this end, tartrate **18** was reduced by DIBALH to the corresponding dialdehyde, which was then reacted in situ with divinylzinc to afford carbinol **19** in a highly stereoselective fashion.<sup>42</sup> Dimethylation and cleavage of the acetonide protecting group with aqueous acid furnished 1,2-diol **20** in excellent yield.<sup>43</sup> The desired  $\alpha$ -methoxy- $\alpha$ -vinyl aldehyde **2** emerged following cleavage of the glycol linkage of **20**. Importantly, no attempts were undertaken to isolate **2** in neat form. Instead, a stock solution of the aldehyde as obtained from the glycol cleavage was directly used for the LACDAC sequence. We were rather encouraged to find that the  $\alpha$ -chelation-controlled cyclocondensation of **2** with butadiene **3** occurred in very good yield, producing dihydropyrone **21** as the only detected diastereomer.

**Scheme 4.** Synthesis of Dihydropyrone **21** by a Cyclocondensation (LACDAC)<sup>a</sup>



<sup>a</sup> Reagents and conditions: (a) DIBALH, then ZnCl<sub>2</sub>, H<sub>2</sub>C=CHMgBr, toluene, –78 °C to room temperature, 75% (ds > 90%); (b) (i) MeI, NaH, DMF, room temperature, (ii) 2 M HCl, MeOH, reflux, 80%; (c) Pb(OAc)<sub>4</sub>, Na<sub>2</sub>CO<sub>3</sub>, CH<sub>2</sub>Cl<sub>2</sub>, 0 °C to room temperature; (d) (i) TiCl<sub>4</sub>, CH<sub>2</sub>Cl<sub>2</sub>, –78 °C, (ii) TFA, CH<sub>2</sub>Cl<sub>2</sub>, room temperature, 87% from **20**.

**Scheme 5.** Synthesis of Key Intermediate **26**<sup>a</sup>



<sup>a</sup> Reagents and conditions: (a) LiBH<sub>4</sub>, MeOH, THF, –10 °C; (b) CSA, H<sub>2</sub>O, THF, reflux; (c) LiBH<sub>4</sub>, H<sub>2</sub>O, THF, room temperature, 53% from **21**; (d) (i) TBSOTf, 2,6-lutidine, CH<sub>2</sub>Cl<sub>2</sub>, room temperature, (ii) HOAc, H<sub>2</sub>O, THF (3:1:1), room temperature, 80%.

Compound **21** not only possesses the three contiguous stereocenters of the macrolide, but it also serves as a template for the construction of the trisubstituted C11–C12 (*Z*)-alkene (Scheme 5). From a process standpoint, it is noteworthy that only two chromatographic purifications were needed to obtain pure **21**, rendering the sequence amenable to scale-up.

Transformation of dihydropyrone **21** into open-chain diol **25** was accomplished as described for our model study (Scheme 3) using a reduction-Ferrier-rearrangement-reductive ring-opening protocol (Scheme 5). Initially, we followed the Luche procedure for the reduction of enones to effect the conversion of **21** to **22**. Subsequently, we found that the addition of cerium salts was not needed in our case. In fact, all of the reductants screened led exclusively to 1,2-reduction. In the end, LiBH<sub>4</sub> turned out to be the reducing agent of choice based on its associated ease of handling and workup. When alcohol **22** was subjected to catalytic amounts of camphorsulfonic acid (CSA) in refluxing aqueous THF, the desired Ferrier-rearranged product **23** was obtained, together with small amounts of dimeric acetal **24**. It is appropriate to note that there are few examples of aqueous Ferrier rearrangements reported in the literature,<sup>44</sup> whereas variants that involve alcohol-based nucleophiles are widely encountered. Reductive opening of lactol **23** with LiBH<sub>4</sub>

(39) Tebbe, F. N.; Parshall, G. W.; Reddy, G. S. *J. Am. Chem. Soc.* **1978**, *100*, 3611–3613.

(40) For initial reports of Grubbs-II catalyst **16**, see: (a) Scholl, M.; Trnka, T. M.; Morgan, J. P.; Grubbs, R. H. *Tetrahedron Lett.* **1999**, *40*, 2247–2250. (b) Scholl, M.; Ding, S.; Lee, C. W.; Grubbs, R. H. *Org. Lett.* **1999**, *1*, 953–956.

(41) For the first report of these new, optimized RCM conditions, see: (a) Yamamoto, K.; Biswas, K.; Gaul, C.; Danishefsky, S. J. *Tetrahedron Lett.* **2003**, *44*, 3297–3299. The same reaction conditions were also applied to the first total synthesis of epothilone 490: (b) Biswas, K.; Lin, H.; Njardarson, J. T.; Chappell, M. D.; Chou, T. C.; Guan, Y.; Tong, W. P.; He, L.; Horwitz, S. B.; Danishefsky, S. J. *J. Am. Chem. Soc.* **2002**, *124*, 9825–9832.

(42) Jorgensen, M.; Iversen, E. H.; Paulsen, A. L.; Madsen, R. *J. Org. Chem.* **2001**, *66*, 4630–4634.

(43) Lee, W. W.; Chang, S. *Tetrahedron: Asymmetry* **1999**, *10*, 4473–4475.

afforded diol **25** in 53% overall yield (from dihydropyrone **21**). In investigating the preparative aspects of the sequence **21** → **25**, we realized that larger amounts of **24** (ca. 15%) were isolated when the Ferrier rearrangement was conducted at higher concentrations (0.3 M instead of 0.1 M). Happily, we were able to obtain single crystals of dimer **24**. X-ray analysis led to a decisive structural verification,<sup>45</sup> revealing the relative configuration of the three contiguous stereocenters and the geometry of the double bond to be as predicted on the basis of our precedents. By extension, this X-ray analysis also confirms the structure of diol **25**.

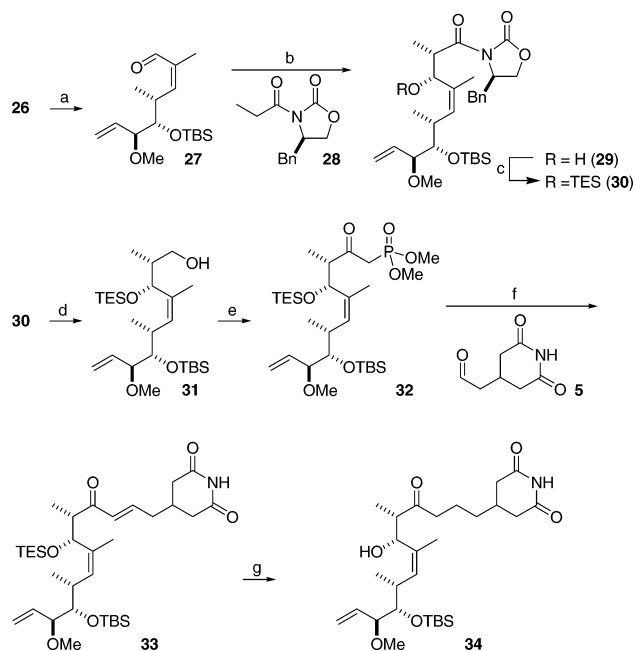
In the next phase of our synthesis of migrastatin, it was necessary to differentiate the two hydroxyl groups of **25**. Previously, we had accomplished this sub-goal via a three-step sequence, acetylation of the primary hydroxyl group, silylation of the secondary hydroxyl group, and subsequent removal of the acetate protecting group.<sup>27</sup> However, during scale-up efforts, we observed the formation of considerable amounts of diacetylated product. This obstacle complicated purification procedures and lowered the overall yield of the sequence. Fortunately, the problem could easily be managed by initial disilylation, followed by a mild and selective deprotection, producing allylic alcohol **26** in 80% yield (Scheme 5).

#### Incorporation of the Glutarimide-Containing Side Chain.

A straightforward way to construct the two remaining stereocenters at C13 and C14 could, in principle, be accomplished by an anti-selective aldol reaction between an aldehyde derived from **26** and an appropriate propionyl fragment. Indeed, Dess–Martin oxidation<sup>46</sup> of **26** generated angelic-type aldehyde **27** (Scheme 6). Fortunately, **27** proved to be notably resistant to (*Z*) → (*E*)-double bond isomerization or vinylogous epimerization and, accordingly, could serve as a potential substrate in the aldol construction. In our early studies, we explored Masamune's anti-aldol protocol, which utilizes a boron enolate of readily available norephedrine derivatives.<sup>47</sup> This aldol reaction indeed worked smoothly with aldehyde **27**. Nonetheless, we were particularly drawn to a mild MgCl<sub>2</sub>-catalyzed anti-aldol procedure that had recently been disclosed by Evans.<sup>48</sup> In practice, aldehyde **27** reacted with propionyl oxazolidinone **28** in the presence of MgCl<sub>2</sub>, triethylamine, and TMSCl to afford, after treatment with TFA, the desired aldol adduct **29** in 67% yield as a single diastereomer. Noteworthy, the robust reaction conditions, which tolerate the use of reagent-grade ethyl acetate and high substrate concentrations, are attractive features for scale-up purposes. Because the next step of the total synthesis was the protection of the C13 hydroxyl group as a TES ether, we tried to accomplish the anti-aldol joining with TESCOI instead of TMSCl. Unfortunately, the reaction was very slow under these conditions, and the yields were far from satisfactory. Hence, we had to protect the secondary hydroxyl group with TESCOI in a separate step (**29** → **30**) (Scheme 6).

Having successfully merged three of our five components, we focused now on attaching glutarimide aldehyde **5** to the main

**Scheme 6.** Incorporation of the Side Chain by an Anti-Aldol Reaction and a HWE Coupling<sup>a</sup>



<sup>a</sup> Reagents and conditions: (a) Dess–Martin periodinane, CH<sub>2</sub>Cl<sub>2</sub>, room temperature; (b) (i) MgCl<sub>2</sub>, Et<sub>3</sub>N, TMSCl, EtOAc, room temperature, (ii) TFA, MeOH, room temperature, 67% from **26**; (c) TESCOI, imidazole, CH<sub>2</sub>Cl<sub>2</sub>, room temperature; (d) LiBH<sub>4</sub>, MeOH, THF, room temperature, 83% from **29**; (e) (i) Dess–Martin periodinane, CH<sub>2</sub>Cl<sub>2</sub>, room temperature, (ii) dimethyl methylphosphonate, BuLi, THF, −78 to 0 °C, (iii) Dess–Martin periodinane, CH<sub>2</sub>Cl<sub>2</sub>, room temperature; (f) LiCl, DBU, MeCN, room temperature, 57% from **31**; (g) (i) [(Ph<sub>3</sub>P)CuH]<sub>6</sub>, toluene, room temperature, (ii) HOAc, H<sub>2</sub>O, THF (3:1:1), room temperature, 82%.

fragment. A Horner–Wadsworth–Emmons (HWE) reaction between β-ketophosphonate **32** and aldehyde **5** appeared to be a plausible, attractive solution to this synthetic problem (Scheme 6). Toward this end, we investigated the direct addition of lithiated dimethyl methylphosphonate to imide **30** to access the desired phosphonate **32** in a single transformation. Unfortunately, this transformation met with no success, resulting in recovery of starting material.<sup>49</sup> Accordingly, the chiral auxiliary was removed reductively (**30** → **31**). Progress continued with a simple and reliable three-step oxidation-addition-reoxidation protocol, cleanly affording phosphonate **32**. Glutarimide aldehyde **5**,<sup>50</sup> the fourth component in our synthetic plan, was then treated with phosphonate **32** using the Masamune–Roush variant of the HWE reaction.<sup>51</sup> Enone **33** was obtained as a single olefin isomer in excellent yield (Scheme 6). Fortunately, neither this reaction nor any of the subsequent transformations required protection of the glutarimide nitrogen. Conjugate reduction of enone **33** with the Stryker reagent<sup>52</sup> and cleavage of the TES protecting group occurred smoothly to give alcohol

(44) (a) Danishefsky, S. J.; Kato, N.; Askin, D.; Kerwin, J. F., Jr. *J. Am. Chem. Soc.* **1982**, *104*, 360–362. (b) Eng, H. M.; Myles, D. C. *Tetrahedron Lett.* **1999**, *40*, 2279–2282.

(45) Crystallographic data (excluding structural data) for compound **24** have been deposited with the Cambridge Crystallographic Data Centre (CCDC) as Deposition No. CCDC 230121.

(46) Dess, D. B.; Martin, J. C. *J. Am. Chem. Soc.* **1991**, *113*, 7277–7287.

(47) Abiko, A.; Liu, J. F.; Masamune, S. *J. Am. Chem. Soc.* **1997**, *119*, 2586–2587.

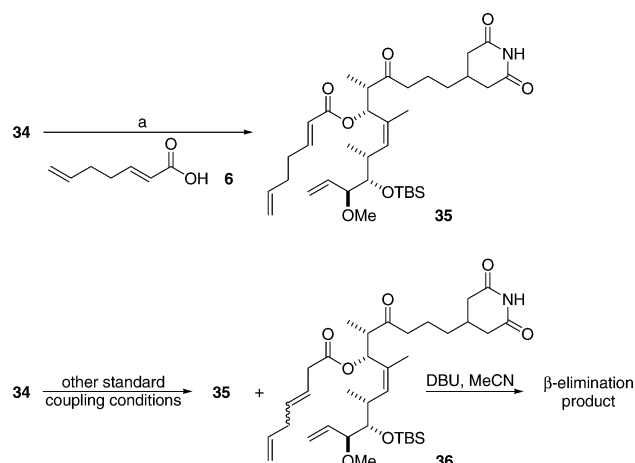
(48) Evans, D. A.; Tedrow, J. S.; Shaw, J. T.; Downey, C. W. *J. Am. Chem. Soc.* **2002**, *124*, 392–393.

(49) For examples of the direct addition of lithiated dimethyl methylphosphonate to esters, see, for example: (a) Edmonds, M. K.; Abell, A. D. *J. Org. Chem.* **2001**, *66*, 3747–3752. (b) Smith, A. B., III; Frohn, M. *Org. Lett.* **2001**, *3*, 3979–3982.

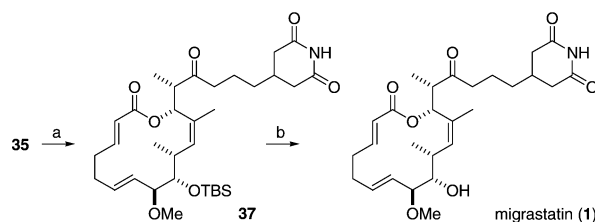
(50) Egawa, Y.; Suzuki, M.; Okuda, T. *Chem. Pharm. Bull.* **1963**, *11*, 589–595.

(51) Blanchette, M. A.; Choy, W.; Davis, J. T.; Essensfeld, A. M.; Masamune, S.; Roush, W. R.; Sakai, T. *Tetrahedron Lett.* **1984**, *25*, 2183–2186.

(52) Mahoney, W. S.; Brestensky, D. M.; Stryker, J. M. *J. Am. Chem. Soc.* **1988**, *110*, 291–293. The Stryker reagent provided by Aldrich performed poorly in the conjugate reduction. The reagent provided by Fluka or prepared by us led to superior results.

**Scheme 7.** Acylation of Alcohol **34** by a Modified Yamaguchi Procedure<sup>a</sup>

<sup>a</sup> Reagents and conditions: (a) 2,4,6-trichlorobenzoyl chloride, *i*-Pr<sub>2</sub>NEt, pyridine, toluene, room temperature, 67%.

**Scheme 8.** RCM and Deprotection Leading to (+)-Migrastatin (**1**)<sup>a</sup>

<sup>a</sup> Reagents and conditions: (a) Grubbs-II catalyst **16** (20 mol %), toluene (0.5 mM), reflux, 69%; (b) HF·pyridine, THF, room temperature, 85%.

**34.** At this stage, the path was clear for introduction of our last component, 2,6-heptadienoic acid **6**.

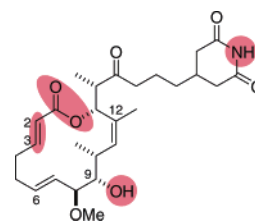
**Completion of the Total Synthesis of Migrastatin.** In our planning stages, we presumed that acylation of secondary alcohol **34** with acid **6** would be straightforward. Unexpectedly, a number of acylation conditions had to be explored to accomplish the desired transformation effectively. Only after extensive experimentation did we find that a modified Yamaguchi acylation protocol<sup>53</sup> (using pyridine instead of DMAP) provided satisfying yields of acylated product **35** (Scheme 7). Most other standard ester formation protocols (a, acid chloride + DMAP, pyridine, or AgCN; b, acid + EDC or DCC; c, acid + Mukaiyama reagent;<sup>54</sup> d, Keck coupling<sup>55</sup>) led to either decomposition of starting material or an inseparable product mixture of **35** and  $\beta,\gamma$ -unsaturated ester **36** (Scheme 7). The latter presumably arose from acylation of **34** with the vinylketene derived from **6** upon activation of the acyl group. Attempts to isomerize the C3–C4 double bond of **36** back into conjugation resulted in loss of the carboxylic acid fragment, apparently through a  $\beta$ -elimination pathway.

With RCM precursor **35** now available, we were positioned to investigate the cyclization reaction (Scheme 8). In the event, the ring-closing metathesis conditions employed in our model system (Scheme 3) also sufficed nicely for the case at hand,

(53) (a) Inanaga, J.; Hirata, K.; Saeki, H.; Katsuki, T.; Yamaguchi, M. *Bull. Chem. Soc. Jpn.* **1979**, *52*, 1989–1993. For a recent example, see: (b) Song, F.; Fidanze, S.; Benowitz, A. B.; Kishi, Y. *Org. Lett.* **2002**, *4*, 647–650.

(54) (a) Mukaiyama, T.; Usui, M.; Shimada, E.; Saigo, K. *Chem. Lett.* **1975**, 1045–1048. (b) Mukaiyama, T. *Angew. Chem., Int. Ed. Engl.* **1979**, *18*, 707–721.

(55) Boden, E. P.; Keck, G. E. *J. Org. Chem.* **1985**, *50*, 2394–2395.

**Figure 2.** Regions of migrastatin targeted for derivatization.

delivering macrolactone **37** in a highly (*E*)-selective fashion in 69% yield. This corresponds to an increase in yield by almost 20% as compared to our model studies! Finally, removal of the TBS protecting group by buffered hydrogen fluoride completed the total synthesis of (+)-migrastatin (**1**), whose physical data (NMR, MS, optical rotation) matched those of migrastatin isolated from natural sources.

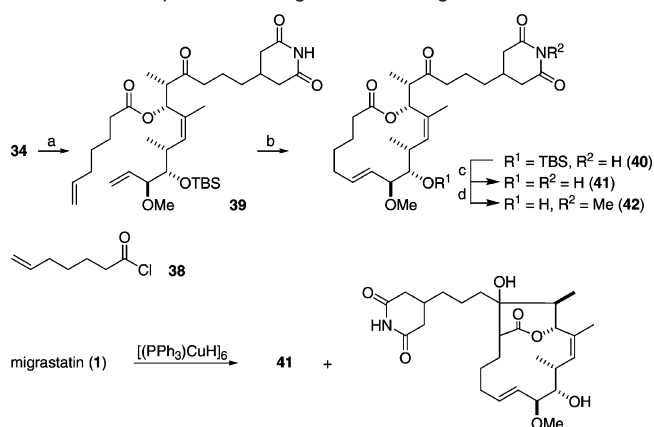
**Design, Chemical Synthesis, and Evaluation of Migrastatin Analogues.** Having achieved the first key goal, the total synthesis of migrastatin, we could take full advantage of our flexible multicomponent synthesis for the subsequent analogue program. As will be evident, our modular approach served as an excellent platform from which to quickly explore the SAR profile of migrastatin and assess the anti-metastatic potential of the migrastatin family.

Our modus operandi in searching for, preparing, and interrogating migrastatin derivatives as to improved cell migration inhibition properties was comprised of three distinct steps: design, chemical synthesis, and biological evaluation. The design of the analogues was aimed at probing the different regions of migrastatin for their contributions to biological activity. The domains of the molecule that we considered important and accessible by synthesis are highlighted in red as shown in Figure 2. The selection was driven by the following considerations: The glutarimide moiety is certainly one the most characteristic functional groups of migrastatin which might be indispensable for activity. The C2–C3 conjugated double bond is a potential site for deactivation by 1,4-addition of nucleophiles (e.g., thiols, confer the natural products NK30424A/B in Scheme 1) or, on the contrary, could render migrastatin a suicide inhibitor by covalent bond formation with bionucleophiles present in the active site of an enzyme. The lactone functionality could possibly be a target of hydrolysis in living systems. As such, manipulation of the ester bond might enhance the in vivo stability of the molecule. Furthermore, the C6–C12 portion of migrastatin is highly functionalized and, thus, might have biological relevance. One simple way of exploring this region is through derivatization of the C9 hydroxyl group.

The chemical synthesis of the analogues was accomplished in an efficient manner by utilizing the concept of diverted total synthesis (DTS).<sup>28</sup> We put to advantage key intermediates of the migrastatin synthesis, such as **26** and **34** (Schemes 5 and 6), as branching points to rapidly assemble a diverse, but still limited, set of migrastatin derivatives. In keeping with the unique capabilities of diverted total synthesis, we focused on target structures that would not have been accessible through manipulations of the natural product itself or through biosynthetic pathways.

The biological evaluation of our compounds (in terms of their ability to inhibit cell migration) was accomplished in a Boyden chamber cell migration assay. In this assay, mouse breast tumor



**Scheme 9.** Preparation of Migrastatin Analogues **41** and **42**<sup>a</sup>

<sup>a</sup> Reagents and conditions: (a) 6-heptenoyl chloride **38**, DMAP, CH<sub>2</sub>Cl<sub>2</sub>, room temperature, 69%; (b) Grubbs-II catalyst **16** (20 mol %), toluene (0.5 mM), reflux, 79%; (c) HF·pyridine, THF, room temperature, 81%; (d) MeI, Cs<sub>2</sub>CO<sub>3</sub>, acetone, 85%.

cells (4T1 cells) or endothelial cells (HUVECs) are seeded on the upper chamber of a transwell insert. Growth factor-containing serum is added to the lower chamber. After incubation for 6–8 h in the presence of different concentrations of our analogues, cells that migrated from the upper chamber through the membrane to the lower compartment are counted. Additionally, some of our more potent compounds were tested for their effect on cell proliferation and metabolic stability in mouse plasma. As will be demonstrated below, the program helped to provide us with a broad SAR picture in the context of our migrastatin studies.

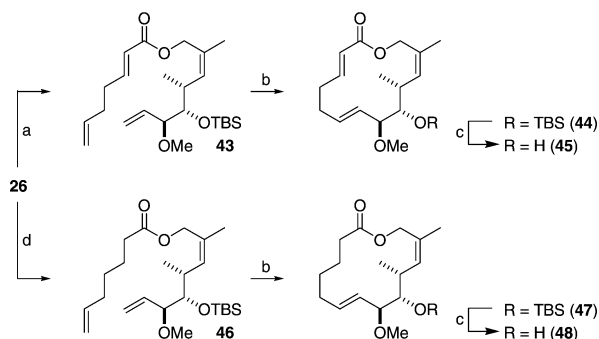
Our search commenced with the synthesis of 2,3-dihydromigrastatin **41** and *N*-methylated 2,3-dihydromigrastatin **42**. Secondary alcohol **34** (Scheme 6), an advanced intermediate of the migrastatin synthesis, was acylated with 6-heptenoyl chloride **38** to deliver RCM precursor **39** (Scheme 9). As expected, acylation proceeded smoothly, without resort to the special reaction conditions required for the acylation of **34** with 2,6-heptadienoic acid **6** (Scheme 7). Compound **39** was cyclized to macrolactone **40** by a very efficient (*E*)-selective RCM. Cleavage of the TBS ether with HF·pyridine yielded our first analogue, 2,3-dihydromigrastatin **41**. Alternatively, compound **41** was prepared directly from migrastatin by regioselective reduction using the Stryker reagent (Scheme 9). The yield of the direct transformation, however, was compromised by the formation of a side product that arose from an intramolecular aldol addition of the transient copper enolate to the C15 ketone. Methylation of the glutarimide nitrogen was accomplished by treatment of **41** with MeI and Cs<sub>2</sub>CO<sub>3</sub> in acetone, delivering methylated 2,3-dihydromigrastatin **42** in excellent yield.

The first set of compounds – migrastatin, together with its analogues **41** and **42** – was then evaluated in the chamber cell migration assay. The IC<sub>50</sub> value for fully synthetic migrastatin with 4T1 tumor cells was 29 μM (Table 1); this result was in excellent agreement with that reported by Imoto for migrastatin obtained from natural sources. Interestingly, reduction of the C2–C3 double bond and methylation of the glutarimide nitrogen were well tolerated with respect to maintenance of activity. Analogues **41** and **42** are actually slightly more potent than migrastatin itself, with IC<sub>50</sub> values of 10 and 7 μM, respectively (Table 1).

**Table 1.** Chamber Cell Migration Assay with 4T1 Tumor Cells

compound	IC <sub>50</sub> (4T1 tumor cells) <sup>a</sup>
migrastatin ( <b>1</b> )	29 μM
2,3-dihydromigrastatin ( <b>41</b> )	10 μM
<i>N</i> -methyl-2,3-dihydromigrastatin ( <b>42</b> )	7.0 μM
migrastatin core ( <b>45</b> )	22 nM
macrolactone ( <b>48</b> )	24 nM
acetylated macrolactone ( <b>49</b> )	192 nM
oxidized macrolactone ( <b>50</b> )	223 nM
hydrolyzed core ( <b>51</b> )	378 nM
macrolactam ( <b>55</b> )	255 nM
macroketone ( <b>60</b> )	100 nM
( <i>S</i> )-isopropyl macrolactone ( <b>65</b> )	227 μM
( <i>R</i> )-isopropyl macrolactone ( <b>68</b> )	146 μM
macrocylic secondary alcohol ( <b>69</b> )	8.9 μM
macrocylic tertiary alcohol ( <b>70</b> )	3.1 μM
macrocylic CF <sub>3</sub> -alcohol ( <b>71</b> )	101 nM
macrooxime ( <b>72</b> )	2.3 μM
biotinylated macrohydrazone ( <b>73</b> )	331 nM
epoxyquinol	26 nM
evodiamine	315 nM

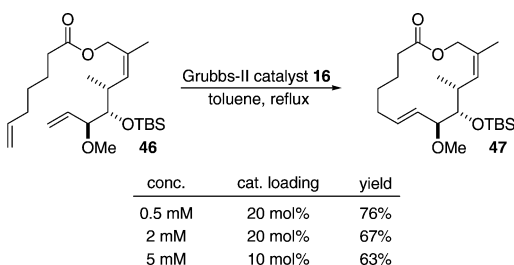
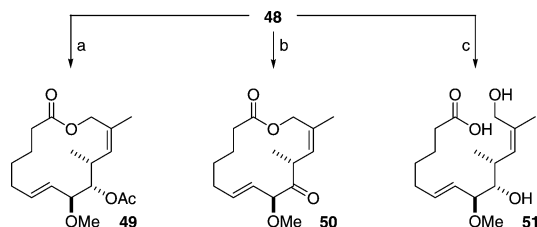
<sup>a</sup> Average of three experiments. Each experiment consists of nine data points (nine different concentrations).

**Scheme 10.** Synthesis of Migrastatin Core **45** and Macrolactone **48**<sup>a</sup>

<sup>a</sup> Reagents and conditions: (a) 2,6-heptadienoic acid **6**, 2,4,6-trichlorobenzoyl chloride, *i*-Pr<sub>2</sub>NEt, pyridine, toluene, room temperature, 48%; (b) Grubbs-II catalyst **16** (20 mol %), toluene (0.5 mM), reflux, 55% (**44**), 76% (**47**); (c) HF·pyridine, THF, room temperature, 66% (**45**), 94% (**48**); (d) 6-heptenoyl chloride **38**, DMAP, CH<sub>2</sub>Cl<sub>2</sub>, room temperature, 82%.

The small change in inhibitory activity upon alkylation of the glutarimide moiety encouraged us to undertake a more drastic structural modification of the migrastatin skeleton. Toward this end, analogues were synthesized lacking the entire glutarimide-containing side chain, migrastatin core **45** and the corresponding reduced version **48** (Scheme 10). Starting from advanced key intermediate **26** (Scheme 5), derivatives **45** and **48** were quickly assembled via the already established acylation-RCM-deprotection sequence. While the reaction of **26** with 2,6-heptadienoic acid **6** produced acylated product **43** in only moderate (48%) yield, the acylation steps in the “dihydro series” occurred smoothly, affording **46** in 82% yield. The same trend was observed for the subsequent transformation, in which the ring closure was achieved in excellent (76%) yield for the saturated case (**46** → **47**). By contrast, the unsaturated core was delivered in lower (55%) yield (**43** → **44**). Finally, protecting group removal delivered macrolactones **45** and **48** without complications.

Given our goal of evaluating the efficacy of migrastatin analogues in animal models, we undertook a brief study of the RCM parameters for a potential large-scale preparation of the macrocycles. The original reaction conditions called for 20 mol

**Scheme 11.** Optimization of the RCM Conditions for Scale-Up Purposes**Scheme 12.** Modification of Macrolactone **48** at the C9 Position and Hydrolysis of **48**<sup>a</sup>

<sup>a</sup> Reagents and conditions: (a) AcCl, DMAP, CH<sub>2</sub>Cl<sub>2</sub>, room temperature, 76%; (b) Dess–Martin periodinane, CH<sub>2</sub>Cl<sub>2</sub>, room temperature, 72%; (c) 0.5 M NaOH, MeOH, room temperature, 77%.

% catalyst at 0.5 mM concentration, but as illustrated for the cyclization of **46** to **47** (Scheme 11), the RCM product could be obtained in just slightly reduced yield by conducting the reaction with 10 mol % catalyst at 5 mM concentration.

Upon examination of compounds **45** and **48** in the cell migration assay, we achieved, to our great surprise, a major breakthrough in potency (Table 1). The IC<sub>50</sub> values for migrastatin core **45** and macrolactone **48** were found to be 22 and 24 nM, respectively. This translates into an increase in activity by 3 orders of magnitude as compared to migrastatin! The assay outcome clearly shows that the migrastatin side chain is not required for in vitro inhibition of tumor cell migration, but it remains to be seen if migrastatin and the core analogues **45** and **48** are indeed directed at the same cellular targets.

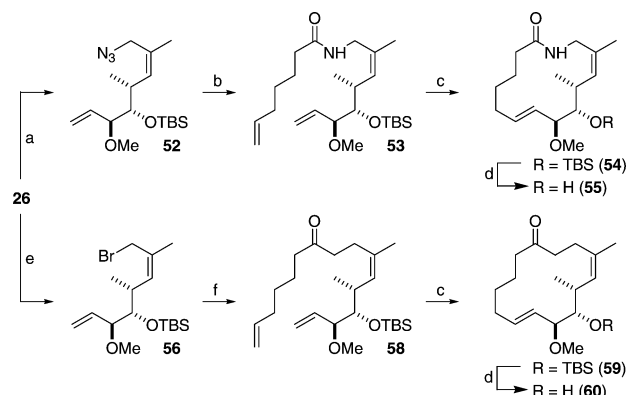
Another potential “hot spot” of migrastatin is the C6–C12 region with its two double bonds, three stereocenters, and two heteroatoms. An easy way of derivatizing this portion of the molecule was found to be the acylation or oxidation of the C9 hydroxyl group, producing macrolactones **49** and **50**, respectively (Scheme 12). As shown in Table 1, the inhibitory activity of analogues **49** and **50** was reduced by roughly an order of magnitude, as compared to macrolactone **48**, indicating that the C9 position is sensitive toward modification.

Starting from our lead compound migrastatin, we were able to reach simplified congeners with drastically improved inhibitory activities, in particular, macrolactones **45** and **48**. Anticipating in vivo evaluation of our compounds, we undertook to evaluate, in a preliminary way, their metabolic stabilities. Based on our experiences from the epothilone program,<sup>56</sup> the ester bond of the macrolactones could well be susceptible toward opening by esterases in mouse (or human) plasma. Such hydrolysis would lead to deactivation of the compound. From this perspective, we undertook to determine the mouse blood plasma stability of migrastatin and the novel analogues **41**, **42**, **45**, and

**Table 2.** Metabolic Stability of Selected Compounds in Mouse Plasma

compound	stability ( <i>t</i> <sub>1/2</sub> , mouse plasma)
migrastatin ( <b>1</b> )	stable <sup>a</sup>
2,3-dihydromigrastatin ( <b>41</b> )	stable <sup>a</sup>
<i>N</i> -methyl-2,3-dihydromigrastatin ( <b>42</b> )	stable <sup>a</sup>
migrastatin core ( <b>45</b> )	20 min
macrolactone ( <b>48</b> )	< 5 min
macrolactam ( <b>55</b> )	stable <sup>a</sup>
macroketone ( <b>60</b> )	stable <sup>a</sup>
( <i>S</i> )-isopropyl macrolactone ( <b>65</b> )	stable <sup>a</sup>
( <i>R</i> )-isopropyl macrolactone ( <b>68</b> )	stable <sup>a</sup>

<sup>a</sup> Intensity of HPLC signal unchanged over 60 min of incubation.

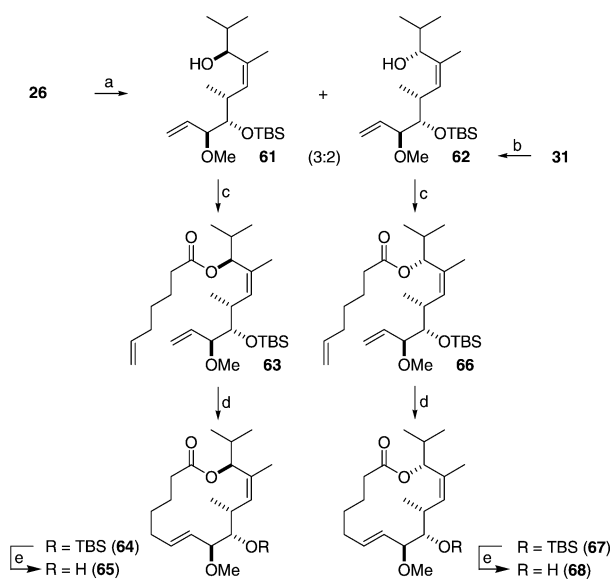
**Scheme 13.** Synthesis of Macrolactam **55** and Macroketone **60**<sup>a</sup>

<sup>a</sup> Reagents and conditions: (a) DPPA (diphenylphosphoryl azide), DBU, toluene, room temperature, 87%; (b) (i) PPh<sub>3</sub>, H<sub>2</sub>O, THF, 70 °C, (ii) 6-heptenoic acid, EDC, *i*-Pr<sub>2</sub>NEt, CH<sub>2</sub>Cl<sub>2</sub>, room temperature, 92%; (c) Grubbs-II catalyst **16** (20 mol %), toluene (0.5 mM), reflux, 60% (**54**), 81% (**59**); (d) HF·pyridine, THF, room temperature, 81% (**55**), 90% (**60**); (e) CBr<sub>4</sub>, solid supported PPh<sub>3</sub>, CH<sub>2</sub>Cl<sub>2</sub>, room temperature; (f) (i) β-keto-sulfone **57**, DBU, toluene, room temperature, (ii) Na/Hg, Na<sub>2</sub>HPO<sub>4</sub>, MeOH, room temperature, 61% from **26**.

**48**. As summarized in Table 2, migrastatin and the side-chain-containing derivatives **41** and **42** were completely inert toward lactone opening over the full test period (1 h). However, the most active compounds, macrolactones **45** and **48**, were hydrolyzed rapidly (Table 2). These findings are not entirely surprising, considering that the ester bonds in **45** and **48** are sterically less congested relative to those in the other analogues. As a test of the “deactivation hypothesis”, the hydrolysis product of macrolactone **48** was prepared (Scheme 12) and tested for its activity against tumor cell migration. Surprisingly, compound **51** was not completely inactive in the chamber assay, but retained a good part of its activity (IC<sub>50</sub> value of 378 nM). Therefore, compound **48** might be effective in the projected in vivo models despite its sensitivity toward hydrolysis. Nevertheless, the data on the unsatisfactory metabolic stability of **45** and **48** influenced us, when we entered the second phase of our analogue program. The aspiration of reaching migrastatin congeners with enhanced plasma stability and retained or improved activity (as compared to **45** or **48**) led to the diverted total synthesis of macrolactam **55**, macroketone **60** (Scheme 13), and the sterically hindered macrolactones **65** and **68** (Scheme 14).

The synthesis of analogues **55**, **60**, **65**, and **68** diverged from the original route to migrastatin at the stage of the advanced key intermediate **26**. For the preparation of lactam **55**, alcohol **26** was subjected to Mitsunobu conditions with DPPA affording allylic azide **52** in 87% yield (Scheme 13).<sup>57</sup> To avoid double

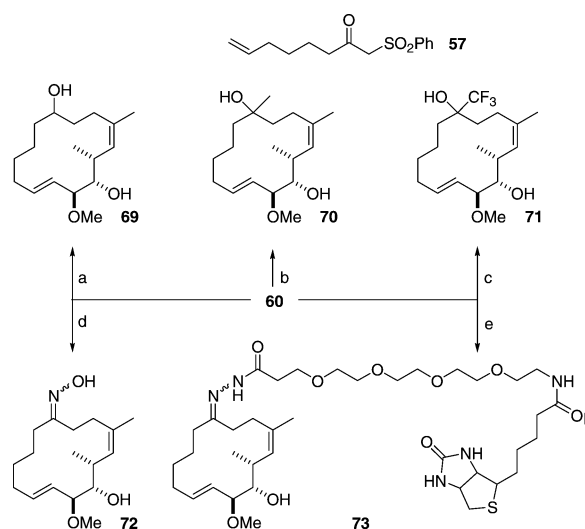
(56) Stachel, S. J.; Lee, C. B.; Spassova, M.; Chappell, M. D.; Bornmann, W. G.; Danishefsky, S. J. *J. Org. Chem.* **2001**, *66*, 4369–4378 (includes an example for the Mitsunobu–Staudinger sequence).

**Scheme 14.** Synthesis of the Diastereomeric Isopropyl Macrolactones **65** and **68**<sup>a</sup>

bond isomerization of the (*Z*)-allylic system, azide **52** was immediately reduced following the Staudinger protocol<sup>57</sup> and subsequently joined with 6-heptenoic acid under standard peptide coupling conditions. The resulting product, amide **53**, was treated with RCM catalyst **16** under our established reaction conditions, delivering lactam **54** in 60% yield. The latter was then deprotected with HF·pyridine to afford lactam **55**.

The preparation of ketone **60** required the conversion of alcohol **26** into allylic bromide **56**, which was displaced by  $\beta$ -ketosulfone **57** (Scheme 13).<sup>57</sup> Subsequent reductive removal of the sulfone group yielded RCM precursor **58**. The ring closure of **58** to the carbocycle was accomplished, again, very efficiently and selectively by RCM. The desired macroketone **60** was obtained following deprotection of **59**.

The synthesis of the isopropyl macrolactones **65** and **68** also commenced from alcohol **26** (Scheme 14). Oxidation of **26** generated the corresponding (*Z*)-enal, which was then treated with *i*-PrMgCl. When the nucleophilic addition was carried out in THF, an equimolar mixture of the desired addition products **61/62** (3:2 ratio) and the reduced product **26** was obtained. It is well documented in the literature that addition of isopropyl-Grignard reagents to hindered substrates must compete with reduction through hydride delivery from the nucleophile.<sup>58</sup> Fortunately, the product ratio could be improved by changing the solvent from THF to Et<sub>2</sub>O. The reduction pathway was almost completely suppressed by slow addition of *i*-PrMgCl to a solution of the aldehyde in Et<sub>2</sub>O, while carefully maintaining the reaction temperature at -78 °C for several hours. The diastereomers **61** and **62** were derivatized as their (*S*)-MPA and

**Scheme 15.** Derivatization of Macroketone **60**<sup>a</sup>

<sup>a</sup> Reagents and conditions: (a) NaBH<sub>4</sub>, MeOH, room temperature, 95%; (b) MeMgBr, THF, 0 °C to room temperature, 95%; (c) TMSCF<sub>3</sub>, TBAF, THF, 0 °C to room temperature, 80%; (d) NH<sub>2</sub>OH·HCl, pyridine, 45 °C, 70%; (e) Biotin-dPEG4-hydrazide, EtOH, 55 °C, 75%.

(*R*)-MPA esters (MPA =  $\alpha$ -methoxyphenylacetic acid) and analyzed by NMR, leading to the assignment of the newly created stereocenter.<sup>59</sup> Major isomer **61** has the “unnatural” (*S*)-configuration, and minor isomer **62** has the “natural” (*R*)-configuration. In addition, the results of the NMR experiment were probed by a degradation study. We were able to transform compound **31** (Scheme 6), a synthetic intermediate of the total synthesis of migrastatin, into minor isomer **62**, thereby delivering convincing proof for the correctness of the configurational assignment. The transformation was accomplished by converting alcohol **31** into its tosylate, reducing the tosylate with LiAlH<sub>4</sub>,<sup>60</sup> and removing the TES protecting group. For the preparation of lactones **65** and **68**, the addition products **61** and **62** were separated and independently acylated (Scheme 14). Intermediates **63** and **66** were then subjected to our RCM conditions, furnishing the macrocycles **64** and **67** in very good yield. Deprotection occurred smoothly and provided the diastereomeric isopropyl lactones **65** and **68**.

Indeed, lateral modification of the vulnerable ester bond of macrolactones **45** and **48** for more robust entities led to the desired effect of enhanced metabolic stability in all four cases: Macrolactam **55**, macroketone **60**, and isopropyl macrolactones **65** and **68** display no sign of degradation in our assay (Table 2). When tested for their ability to inhibit 4T1 cell migration, compounds **55** and **60** were found to be considerably more active than the natural product migrastatin (255 and 100 nM, respectively, Table 1), although some loss of potency relative to lactones **45** and **48** was recorded. Surprisingly, incorporation of an isopropyl group at C13 proved to be deleterious for biological function. Isopropyl macrolides **65** and **68** exhibited only very weak effects on tumor cell migration (Table 1).

As depicted in Scheme 15, our SAR studies were further diverted on the basis of macroketone **60**. The ketone functionality proved to be an attractive handle for additional derivatization.

(57) Chun, J.; Li, G.; Byun, H. S.; Bittman, R. *J. Org. Chem.* **2002**, *67*, 2600–2605.

(58) For a recent example, see: Dixon, D. J.; Krause, L.; Ley, S. V. *J. Chem. Soc., Perkin Trans. 1* **2001**, 2516–2518.

(59) (a) Trost, B. M.; Bunt, R. C.; Pulley, S. R. *J. Org. Chem.* **1994**, *59*, 4202–4205. (b) Seco, J. M.; Latypov, S. K.; Quinoa, E.; Riguera, R. *Tetrahedron* **1997**, *53*, 8541–8564. (c) Seco, J. M.; Quinoa, E.; Riguera, R. *Tetrahedron: Asymmetry* **2000**, *11*, 2781–2791.

(60) Li, D. R.; Xia, W. J.; Shi, L.; Tu, Y. Q. *Synthesis* **2003**, 41–44.

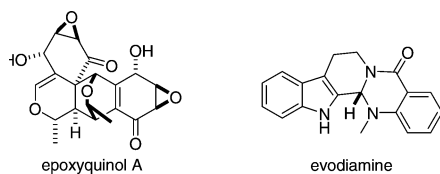


**Figure 3.** Structures of epoxyquinol A and evodiamine.

**Table 3.** Chamber Cell Migration Assay with Human Endothelial Cells (HUVECs)

compound	IC <sub>50</sub> (HUVEC) <sup>a</sup>
migrastatin ( <b>1</b> )	65 $\mu$ M
migrastatin core ( <b>45</b> )	150 nM
macrolactone ( <b>48</b> )	125 nM
macrolactam ( <b>55</b> )	18 $\mu$ M
macroketone ( <b>60</b> )	12 $\mu$ M

<sup>a</sup> Average of three experiments. Each experiment consists of nine data points (nine different concentrations).

We started our explorations by adding various nucleophiles to the carbonyl functionality accessing analogues **69–71**. Simple NaBH<sub>4</sub> reduction of **60** afforded secondary alcohol **69** as a mixture of diastereomers, while addition of MeMgBr gave the corresponding tertiary carbinol mixture **70**. Following a procedure by Olah,<sup>61</sup> nucleophilic addition of a trifluoromethyl group to **60** was accomplished using (trifluoromethyl)trimethylsilane (TMSCF<sub>3</sub>) and catalytic amounts of Bu<sub>4</sub>NF (TBAF). This treatment produced the TMS-protected alcohol intermediate, which was transformed into **71** upon prolonged exposure to TBAF (compound **71** was isolated as a single diastereomer after chromatography). Traditional functionalities, such as in oxime **72**, could also be easily incorporated starting from macroketone **60**. As a part of our long-term goal of elucidating the cellular target of migrastatin and our new migrastatin scaffolds, we condensed commercially available Biotin-dPEG<sub>4</sub>-hydrazide with ketone **60** furnishing the biotin-labeled acyl-hydrazone **73**.

Derivatives **69–73** were evaluated for their ability to inhibit tumor cell migration in the chamber assay. Interestingly, the substitution of the ketone functionality for a more polar group, such as an alcohol or oxime function, seems to be detrimental for the activity. Secondary alcohol **69**, tertiary alcohol **70**, and oxime **72** are rather weak cell migration inhibitors, with IC<sub>50</sub> values of 8.9, 3.1, and 2.3  $\mu$ M, respectively (Table 1). It appears that incorporation of a trifluoromethyl group can compensate for the loss of activity caused by the hydroxyl group: Macrocyclic CF<sub>3</sub>-alcohol **71** displays the same activity profile as macroketone **60**. Gratifyingly, inhibitory potency is largely retained in biotinylated hydrazone **73**. Therefore, system **73**, although a mixture of geometric isomers, could qualify as a probe to assist in the target identification process.

As discussed above, there are other recently discovered natural products that are reported to be strong cell migration inhibitors. In particular, two compounds, epoxyquinol A,<sup>12</sup> a pentaketide dimer with anti-angiogenic activity, and evodiamine,<sup>15</sup> a potent anti-metastatic and anti-invasive alkaloid, attracted great interest and are currently under serious investigation by several research groups (Figure 3). We regarded it as a valuable experiment to test these natural products side by side with our migrastatin analogues for the purpose of validating and calibrating our assay. As shown in Table 1, our simple macrolactones outperform evodiamine and are comparable to epoxyquinol A in the chamber assay.

Due to the significance of endothelial cell migration in the angiogenesis process, the chamber cell migration assay described above was also conducted with HUVECs (human umbilical vein endothelial cells) and used for the evaluation of our most potent analogues, macrolactones **45** and **48**, macrolactam **55**, and macroketone **60**, together with migrastatin as a reference. The IC<sub>50</sub> values obtained from this study are listed in Table 3. The general trend in activity, with the simplified analogues **45**, **48**, **55**, and **60** being significantly more active against 4T1 tumor cell migration than the parent natural product, was also observed for endothelial cells. However, some erosion of potency in the HUVEC determination as compared to the 4T1 cell determination was observed for all compounds tested.

To complete the in vitro mouse assay data set for our analogues, we examined the effect of migrastatin and our front line cell migration inhibitors **48**, **55**, and **60** on 4T1 cell proliferation. Macrolactone **48**, macrolactam **55**, and macroketone **60** did not have any cytotoxic or anti-proliferative effects up to 20  $\mu$ M, whereas migrastatin turned out to be a weak proliferation inhibitor (IC<sub>50</sub> value of 42  $\mu$ M). Gratifyingly, this outcome allows one to conclude that cell proliferation inhibition is not a contributor to the effects observed in the chamber assays, rendering our migrastatin analogues specific for cell migration inhibition.

To translate the murine findings into a human cancer setting, four solid human tumor cell lines and four liquid cancer cell lines were investigated with respect to the inhibitory potential of the most potent compounds macrolactone (**48**), macroketone (**55**), and macrolactam (**60**). Intriguingly, a very high selectivity between the various tumor cell lines was detected (Table 4 and Figure 4). (+)-Migrastatin (**1**) did not respond well to any of the cell lines tested. As stated above, nontransformed human cells as HUVEC appear to be largely more resistant to the compounds. In contrast, three of our tested cell lines (HT 29, Ovar3, and RL) clearly demonstrate a very sensitive response in terms of migration inhibition, without interfering with cell proliferation. Surprisingly, the highly metastatic human breast

**Table 4.** Chamber and Wound-Healing Cell Migration Assay for Various Human Cancer Cells<sup>a</sup>

	HT 29	HCT 116	IGROV	Ovar3	RL	RPMI8226	CAG	MDA MB435
<b>48</b>	13 $\pm$ 3	60 $\pm$ 12	76 $\pm$ 4	20 $\pm$ 2	38 $\pm$ 6	88 $\pm$ 5	89 $\pm$ 12	68 $\pm$ 7
	+	+	+	+	n.d.	n.d.	n.d.	+
<b>55</b>	106 $\pm$ 3	165 $\pm$ 18	101 $\pm$ 3	55 $\pm$ 10	75	82 $\pm$ 7	96 $\pm$ 5	112 $\pm$ 6
	–	–	–	+	n.d.	n.d.	n.d.	–
<b>60</b>	95 $\pm$ 9	104 $\pm$ 2	91 $\pm$ 5	65 $\pm$ 13	85 $\pm$ 12	92 $\pm$ 7	94 $\pm$ 6	98
	–	–	–	+	n.d.	n.d.	n.d.	–

<sup>a</sup> Note: The first number represents percent (%) of uninhibited cells as determined by a chamber cell migration assay, and the plus/minus sign refers to a successful (+) or unsuccessful (–) inhibition of cell migration as determined by a wound-healing assay, n.d. = not done. Concentrations of compounds employed: 10X IC<sub>50</sub>, **48** (240 nM), **55** (1000 nM), **60** (2550 nM). None of the compounds responded to the human breast cancer cell line MCF-7.

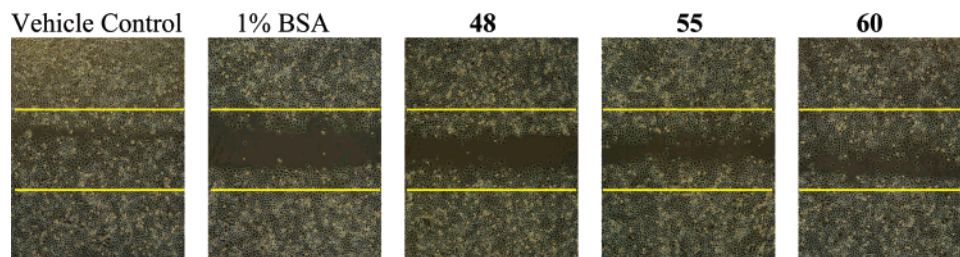


**Figure 4.** Wound-healing cell migration assay results for ovarian cancer cell line Ovarc3. Note: Concentrations of compounds employed: 10X IC<sub>50</sub>, **48** (240 nM), **55** (1000 nM), **60** (2550 nM).

cancer cell line MDA MB435 responded only slightly to **48**, but not at all to **55** and **60**.<sup>62</sup> This was an unforeseen discovery, especially in light of the great response found to these compounds to the 4T1 mouse breast cancer cell line. These findings suggest a highly specific effect on selective cancerous cells, primarily ovarian (Ovarc3) and colon (HT 29) cancers, in comparison to nontransformed cells, indicating a large window for possible therapeutic approaches. In pursuing these data, compound **48** emerges as a particularly appropriate candidate for preclinical development.

### Summary

In conclusion, the total synthesis of migrastatin has been accomplished in a highly convergent way. Key to our successes in the synthesis was the melding of several key reactions. Thus, the powers of the LACDAC reaction (see **2** + **3** → **21**) to control functionality and stereochemistry were interfaced with the Ferrier rearrangement (see **22** → **23**) to fully exploit the resultant pyran matrix. This combination of transformations set the stage for the RCM reaction to establish the macrolactone.

Moreover, recourse to migrastatin as a lead structure, in the context of the modality of diverted total synthesis, created a small, but focused collection of migrastatin analogues, leading to the discovery of a series of highly potent cell migration inhibitors. Our most promising candidates **45**, **48**, **55**, **60**, and **71** are structurally simplified relative to migrastatin and are

easily accessible in large quantities through efficient synthesis. They exhibit favorable properties in cell migration, proliferation, and degradation assays. We are now well positioned to study their efficacy in mouse and human in vivo tumor metastasis models to learn more about their pharmacological profiles in living systems. One of our goals will be the evaluation of these new agents in combination with long-term, low-dose (metronomic) chemotherapy. We anticipate building upon these findings in the context of exploring the migrastatin-based estate in clinical settings.

**Acknowledgment.** This work was supported by grants from the NIH (S.J.D. and X.-Y.H.). Postdoctoral support is gratefully acknowledged by C.G. (Deutscher Akademischer Austauschdienst, DAAD) and J.T.N. (General Motors Cancer Research Program). We thank Dr. Louis Todaro (Hunter College New York) for X-ray structure analyses and Dr. George Sukenick, Ms. Sylvi Rusli, and Ms. Anna Dudkina (NMR Core Facility, Sloan-Kettering Institute, CA-02848) for mass spectral analyses. We are grateful to Professor John A. Porco, Jr. (Boston University) for supplying us with a sample of epoxyquinol A and to Professor Yueming Li (Sloan-Kettering Institute) for helpful discussions.

**Supporting Information Available:** Full experimental details and physical data for all new compounds. Description for the biological assays employed. This material is available free of charge via the Internet at <http://pubs.acs.org>.

(61) Prakash, G. K. S.; Krishnamurti, R.; Olah, G. A. *J. Am. Chem. Soc.* **1989**, *111*, 393–395.

(62) MCF-7, another human breast cancer cell line, did not respond at all.

JA048779Q